(4)

FINAL REPORT

on

ONR Contract N00014-82-K-0084
Period 12/01/81 - 9/30/88

submitted to

Office of Naval Research
Ballston Tower No. 1
800 N. Quincy St.
Arlington, Virginia 22217-5000

Attn: Mike Reischman
Code 1132F

by

Department of Aerospace Engineering
University of Southern California
Los Angeles, California 90089-1191

Co-Principal Investigators:
Blackwelder, Ron
Browand, Frederick
Ho, Ching-Ming
Maxworthy, Tony

Turbulence in Rotating (and/or) Stratified Fluids
(Task 1)

Co-Principal Investigators:
Tony Maxworthy
Frederick Browand

The Departments of Aerospace Engineering and Mechanical Engineering at the University of Southern California acknowledge support from the Office of Naval Research under contract number N00014-82-K-0084 for the period December 1, 1981 through September 30, 1988. The overall objective of the research was (and continues to be) to understand through laboratory experiments, theoretical analyses, and comparisons with field data, the processes by which turbulence in the world's oceans is generated, evolves and decays. Laboratory studies are judiciously chosen to illustrate fundamental processes. Efforts are made to relate the results of laboratory studies to the ocean environment.

During the seven years of the contract period, a total of 56 published articles have appeared in journals or conference proceedings. In addition, two reports have been prepared and given wide circulation within the research community. Highlights of work during the contract period are the following.

I. 1. Comprehensive studies of wave motions in rotating flows, stratified flows, and rotating/stratified flows:

Wave motions are important in transporting momentum and energy within the oceans and atmosphere. The laboratory studies have served to deepen and extend the understanding of such waves. We were the first to describe solitary wave motions on concentrated vortex cores. A series of fundamental experiments have embraced a wide range of applications including: the dynamics of severe storms in the atmosphere, and the quantized vortex motion in liquid Helium. Solitary Kelvin waves -- long wave motions present in all the world's oceans -- were first studied in the laboratory here. The mechanism for tidal generation of internal gravity waves (common features of all continental shelf regions) was also first proposed and studied here.

II. 2. Dynamics of gravity currents:

The first studies of axisymmetric internal gravity currents were carried out at USC, as well as the first studies of gravity currents having a variable rate of supply. Both these circumstances are more typical of naturally occurring gravity currents, and are therefore important.

III. 3. Effect of stratification upon the structure of oceanic turbulence

Turbulence in the ocean must, as a result of the stratification of the medium, continuously lift heavy fluid (from below) and depress lighter fluid (from above). A consequence is that vertical scales of turbulence are limited in extent. We have demonstrated this limiting scale in several dramatic experiments.

The turbulent eddies continue to evolve and spread in the horizontal direction, producing a collection of pancake-shaped structures. This two dimensional (or quasi-two dimensional) turbulent eddy field is characteristic of the ocean at scales from hundreds of meters to hundreds of kilometers. Much of our recent effort has gone into understanding the evolution of this complex field.

IV. 4. The common features of frontal motions/coastal upwelling:

The major fisheries of the world occur in regions of upwelling. The two ingredients are a coast line adjacent to deep water and an along-shore wind field. Ekman flux in the surface boundary layer →

produces upwelling along the coast. Studies in our laboratory show the propagation of waves along the upwelling front, and often a subsequent instability and break-up into off-shore jets. The resulting structure is highly dependent upon the local topography. These frontal instabilities are one source of the two dimensional turbulent eddies mentioned in III. The laboratory studies yield scaling laws which are applicable to the oceanic counterparts. Fractal geometry is employed here for the first time, as a means of clarifying the motion and to characterize the degree of mixing.

V. 5. Fundamental structure of turbulent flows

In addition to studies of oceanic turbulence, we also investigate fundamental issues on the nature of turbulence. These experiments are more easily accomplished in homogeneous (unstratified) flows, although the results have broad application to all turbulent flows. We were the first to emphasize the geometrical characterization of vortex motions in free shear flows. We have identified certain defect features which seem to be fundamental to all unbounded shear flows, and have devised a way to produce and study these defects artificially.

VI. 6. Development and implementation of image processing algorithms

The two published reports deal with the general problem of particle tracking in fluids. The particles may be floats in the ocean or neutrally bouyant particles added to a laboratory flow for the purpose of visualizing the fluid motion. Several tracking and grid interpolation schemes were evaluated in the report, and form the basis of a free software package which is included with the report on a 5¼ inch floppy disk.

Index of Publications

I. Comprehensive studies of wave motion

1. "Turbulence and Waves in a Rotating, Turbulent Flow", with F. Browand and E.J. Hopfinger, J. Fluid Mech., 125, pp. 505-534, 1982.

2. "Vortex Solitary Waves in a Rotating Turbulent Flow", with F. Browand and E.J. Hopfinger, Nature, 295, February 1982.

3. "The Dynamics of Confined Vortices", with T. Maxworthy, M. Escudier and J. Bornstein, Proc. Roy. Soc., Ser. A, p. 335, 1982.

4. "Observations of Inertial Waves in a Homogeneous, Rotating Fluid", with T. Maxworthy and K. Heikes, J. Fluid Mech., 125, p. 319, 1982.

5. "Experiments on Solitary, Internal Kelvin Waves", T. Maxworthy, J. Fluid Mech., 129, pp. 365-383, 1983.

6. "On the Generation and Evolution of Internal Gravity Waves", with T. Maxworthy and F. Lansing, J. Fluid Mech., 145, p. 124, 1984.

7. "Wave Motions on Vortex Cores", with T. Maxworthy, E.J. Hopfinger and L.G. Redekopp, J. Fluid Mech., 151, pp. 141-165, 1985.

8. "Solitary Waves on Density Interfaces", T. Maxworthy, Proc. of Conference on "Waves on Interfaces", Madison, Wisconsin, October 1982.

9. "Dynamics of the Great Red Spot Inferred from Voyager I and II Images", with T. Maxworthy and J.L. Mitchell, submitted to ICARUS.

10. "Waves on Vortex Cores and Their Relationship to Vortex Breakdown", with T. Maxworthy, M. Mory and E.J. Hopfinger, Proc. AGARD Mtg. on Vortex Flows, Brussels, 1983.

11. "Internal Wave Generation and Propagation in a Rotating-Stratified Fluid", with T. Maxworthy, G. Chabert d'Hieres and H. Didelle, J. Geophys. Res., 89, pp. 6383- 6396, 1984.

12. "The Generation of Kelvin Waves by Tidal Flow over Bottom Topography in a Narrow Channel", with T. Maxworthy and Y.N. Liu, J. Geophys. Res., 90, pp. 7235-7242, 1985.

13. "Wave Motions on Concentrated, Columnar Vortices", T. Maxworthy, M. Kruskal Festschrift, Special issue of Physica D, 18, p. 149, 1986.

14. "Waves on Vortex Cores", T. Maxworthy, Proc. IUTAM Symp. on "Fundamental Aspects of Vortex Motion", Tokyo, August 31-September 4, 1987, (Invited lecture).

II. Dynamics of gravity currents

1. "The Viscous Spreading of Plane and Axisymmetric Gravity Currents", with T. Maxworthy and N. Didden, J. Fluid Mech., 121, p. 27, 1982.

2. "The Dynamics of Double-Diffusive Gravity Currents", T. Maxworthy, J. Fluid Mech., 128, pp. 259-282, 1983.

3. "Gravity Currents with Variable Inflow", T. Maxworthy, J. Fluid Mech., 128, pp. 247-257, 1983.

III. Effect of stratification upon the structure of oceanic turbulence

1. "Selective Withdrawal and Spin-up of a Rotating, Stratified Fluid", with T. Maxworthy and S. Monismith, accepted for publication in J. Fluid Mech.

2. "Fractal Geometry in the Energy and Vorticity Fields in Decaying 2D Grid Turbulence", with T. Maxworthy, G. Spedding and Ph. Caperan, submitted to J. Geophys. Res.

3. "Interaction de Tourbillons Bidimensionelle de Meme Signe: Etude Experimentale et Numerique", with T. Maxworthy, Ph. Caperan, J. Verron and E.J. Hopfinger, Proc. of Colloquium "Dynamique de fluides Geophysiques et Astrophysiques", Grenoble, France, September, 1987.

4. "The Stratified Mixing Layer", with F. Browand, G.A. Lawrence and J.C. Lasheras, 6th Conference on Turbulent Shear Flows, Toulouse, France, August 1987.

5. "The Evolution of Grid-Generated Turbulence in the Neighborhood of a Density Step", with F. Browand, R. Amen and T. Maxworthy, for the IAHR 3rd Symposium on Stratified Flow, Cal. Tech., Pasadena, CA, Feb. 3-5, 1987, published Proceedings.

6. "Shear Instabilities in Stratified Flow", with F. Browand, G.A. Lawrence and J.C. Lasheras, for the IAHR 3rd Symposium on Stratified Flow, Cal. Tech., Pasadena, CA, Feb. 3-5, 1987, published Proceedings.

7. "The Behavior of a Turbulent Front in a Stratified Fluid: Experiments with an Oscillating Grid", with F. Browand, D. Guyomar and S.-C. Yoon, for the IUTAM Symposium on Mixing in Stratified Fluids, Margaret River, Western Australia, August 25-29, 1985, Also discussed at APS, Division of Fluid Dynamics Meeting, Tucson, Arizona, Nov. 1985. J. Geophys. Res., Vol. 92, pp. 5329-5341, 1987.

8. "Quasi 2-D Turbulence and Vortices in a Stratified Fluid", with T. Maxworthy, Ph. Caperan and G.R. Spedding, 3rd Int. Conf. on Stratified Flows, Caltech 1987.

9. "Collapse of a Turbulent Front in a Stratified Fluid. Part I. Nominally Two-Dimensional Evolution in a Narrow Tank", with T. Maxworthy, Y.N. Liu and G.R. Spedding, J. Geophys. Res., 92, pp. 5427-5433, 1987.

10. "The Structure of Meso-Scale Baroclinic Turbulence", with T. Maxworthy, S. Narimousa and G.R. Spedding, Sixth Conference on Turbulent Shear Flows, Toulouse, France, August 1987.

11. "An Experimental Investigation of the Coalescence of Two-Dimensional, Finite-Core Vortices", with T. Maxworthy and Ph. Caperan, submitted to J. P. O.

12. "Experiments in Two-Dimensional Turbulence: the Interaction and Merging of Vortices", with T. Maxworthy, Ph. Caperan and G.R. Spedding, Proc. Inter. Conf. on Fluid Mechanics, Beijing, China, July 1987.

13. "The Effects of Rotation on Selective Withdrawal from a Density-Stratified Reservoir", with T. Maxworthy and S. Monismith, 3rd Int. Symp. on Stratified Flows, Caltech 1987.

14. "A Note on Turbulent Mixing Across a Density Interface in the Presence of Rotation", T. Maxworthy, J. Phys. Ocean., 16, p. 1136, 1986.

15. "Natural Flow Visualisation in Lake Eyre", with T. Maxworthy, J. Bye, R. Byron-Scott and R. Nunes, EOS 67, No. 5, South Australia, Feb. 4, 1986.

16. "The Fluid-Dynamics of Natural Phenomena", T. Maxworthy, 10th U. S. National Congress of Applied Mechanics, to appear in A.S.M.E. Trans., 1986. Invited lecture.

17. "Differential Mixing in a Stratified Fluid", with T. Maxworthy, and S. Monismith, J. Fluid Mech., 189, pp. 571-598, 1988.

18. "Differential Deepening of a Mixed Layer in a Stratified Fluid", T. Maxworthy, I.A.H.R. 21st Congress, Melbourne, Australia, August 1985.

19. "The Inhibition of Vertical Turbulent Scale" with F. Browand and E.J. Hopfinger, IMIA Conference Proceedings on Models of Turbulence and Diffusion in Stably Stratified Regions of the Natural Environment, Cambridge, England, March 14-15, 1983.

IV. The common features of frontal motions/coastal upwelling

1. "Laboratory Models of Oceanic Fronts", T. Maxworthy, 4th Asian Conference on Fluid Mechanics, Hong Kong, September 1989. Also submitted to J. of Marine Research.

2. "Fingering Instability at High Flow Rates in a Hele-Shaw Cell", with T. Maxworthy, G.R. Spedding and J. Wiggert, in preparation for J. Fluid Mech.

3. "An Experimental Study of Interface Instability in a Hele-Shaw Cell", T. Maxworthy, 1st Caribbean Conf. on fluid Dynamics, Univ. of the West Indies, Trinidad, January 1989. Also submitted to Phys. Rev. A

4. "The Non-linear Growth of a Gravitationally Unstable Interface in a Hele-Shaw Cell", T. Maxworthy, J. Fluid Mech., 177, pp. 207-232, 1987. Also a note in Phys. Fluids, 28, p. 2637, 1985 (1st Prize A.P.S.-D.F.D. Photo Competition).

5. "Coastal Upwelling on a Sloping Bottom: The formation of jets, plumes and pinched-off cyclones", with T. Maxworthy and S. Narimousa, J. Fluid Mech., 176, pp. 169-190, 1987.

6. "Coastal Upwelling Driven by a Discontinuous Stress Distribution in the Presence of Bottom Topography", with T. Maxworthy and S. Narimousa, J.P.O., 16, pp. 2072-2083, 1986.

7. "The Laboratory Modelling of Coastal Upwelling", with T. Maxworthy and S. Narimousa, Oceanography Report Section of EOS 67, No. 1, January 7, 1986.

8. "Bubble Formation, Motion and Interaction in a Hele-Shaw Cell", T. Maxworthy, J. Fluid Mech. G.I. Taylor Special Volume, December 1986.

9. "Experiments in a Hele-Shaw Cell", T. Maxworthy, in Experiments in Fluid Dynamics, ed. R.C. Granger, 1986.

10. "Experiments and Observations on the Effects of Bottom Topography on Coastal Upwelling, with T. Maxworthy and S. Narimousa, Proc. of Conf. on Vertical Motion in the Tropical Oceans, Paris, May 1985.

11. "The Formation of Tidal-Mixing Fronts", T. Maxworthy, Ocean Modelling, No. 55, March 1984.

12. "A Two-Layer Model of Shear Driven Coastal Upwelling in the Presence of Bottom Topography", with T. Maxworthy and S. Narimousa, J. Fluid Mech., 159, pp. 503-531, 1985.

V. Fundamental structure of turbulent flows

1. "Pattern Evolution in the Two-Dimensional Mixing Layer", with F. Browand and S. Prost-Domasky, NATO Workshop, New Trends in Non-linear Dynamics and Pattern Forming Phenomena: The Geometry of Non-equilibrium, Cargese, France, August 2-12, 1988, Proceedings to be published in Physica D.

2. "A Technique for Acoustic Excitation of Separated Shear Flows: Preliminary Results", with F. Browand and S. Prost-Domasky, Proceedings of the ASME Winter Meeting, Chicago, Illinois, November 28-December 2, 1988.

3. "Forced, Unbounded Shear Flows", with F. Browand and C.M. Ho, invited talk, CHAOS '87, Monterey, CA, January 15, 1987, Nuclear Physics: B, Proceedings Supplement 2, pp. 139-158, 1987.

4. "The Structure of the Turbulent Mixing Layer", F. Browand, Physica 18D, pp. 135-148, 1986. (Invited presentation, International Conference on Solitons and Coherent Structures).

5. "An Experimental Study of Entrainment, Mixing and Chemical Reaction in a Plane Turbulent Shear Layer", with T. Maxworthy, J.C. Lasheras and J.S. Cho, Proceeding of the 20th International Symp. on Combustion, August, 1984.

6. "The Origin of Three-Dimensional Vortical Structures in a Plane, Free-Shear Layer", with T. Maxworthy, J.C. Lasheras and J.S. Cho, J. Fluid Mech., 1986.

7. "The Turbulent Mixing Layer: Geometry of Large Vortices", with F. Browand and T.R. Troutt, J. Fluid Mech, 158, pp. 489-509, 1985.

8. "The Mixing Layer: An Example of Quasi Two-Dimensional Turbulence", with F. Browand and C.M. Ho, Journal de Mecanique Theorique et Appliquee, pp. 99-120, Special Issue 1983.

Index of Reports

VI. Development and Implementation of Image Processing Algorithms

1. "Performance Analysis of Automated Image Processing and Grid Interpolation Techniques for Fluid Flows", with E.J.M. Rignot and G.R. Spedding, USCAE 143, 1988.

2. "Application of Neural Networks to Three-Dimensional Particle Tracking in Fluid Flows", E.J.M. Rignot, USCAE 146, 1988.

CONTROL OF MIXING IN FREE SHEAR LAYERS
(Task 2)

Principal Investigator: Ho, Chih-Ming

ABSTRACT

The main thrust of the research is to understand the physics of the coherent vortices and to develop techniques of controlling the evolution of the deterministic structures. Fundamental understanding of the entrainment and the small scale mixing processes in free shear layers have been obtained during the research period 12/01/81 - 9/30/88.

ACCOMPLISHMENTS

I: Control of 2-D Coherent Structures

The coherent structures are developed from the Kelvin-Helmholtz instability and therefore are sensitive to the initial perturbations. We have found that the almagamation pattern of the vortices can be altered dramatically by perturbing the shear layer at the subharmonics of the most amplified frequency [Ref. I-1,2,3,5, and 6].

The momentum [Ref. I-4] and the mass [Ref. I-3, 5] transfers across the two streams of a free shear layer are caused mainly by the unsteady evolution of the vortices. Hence, the manipulation of the vortex merging patterns has important implications for many technical applications.

II: Instrumentation

The split film probe was a common instrument for simultaneously measuring the streamwise and the transverse velocity components. When it was used in our laboratory, we could never obtain satisfactory results. After a careful examination, we have conclusively shown that the cross-talk between the two films ruined the phase information between the two velocity components. Therefore, the split film probe is not a usable instrument [Ref. II-1].

III: Lock-on of Wake Flow

When a wake was forced by a monochromic disturbance, the wake instability waves locked to the forcing at a certain frequency band. We have identified the ratio between the forcing frequency and the most amplified frequency of the wake as the important parameter for characterizing the lock-on band [Ref. III-1].

IV: Subharmonic Resonance

When the free shear layer was forced by a single frequency, many flow quantities could be predicated by the linear instability analyses. When the flow was perturbed by the fundamental and the subharmonic, the amplification rate of the subharmonic was found to be a function of the phase angle between the fundamental and the subharmonic[Ref. IV-1]. This phenomenon supports the non-linear subharmonic resonance mechanism proposed by Kelly [1967].

V: Streamwise Vortices

The vorticity of streamwise vortices was found to be in the same order of the maximum mean shear of the mixing layer. Furthermore, the wavelength of the streamwise vortices doubled after the merging of the spanwise structures took place [Ref. V-1,2]. The increase of the length scale has been confirmed by the Navier-Stokes numerical simulation [Ref. V-3].

VI: Phase Decorrelation

Near the trailing edge of the splitter plate, the phase of the passing coherent structures has a definite relationship with the forcing signal. The phase jitter was significantly increased after the vortex merging [Ref. VI-1,2]. The phase dynamics and the small scale transition were considered as possible candidates for the phase decorrelation. After a careful examination, we have identified the background noise as having an influence on the growth of the subharmonic. Therefore, we can conclude that the phase decorrelation starts with the vortex merging.

VII: Mixing Transition

In an originally laminar plane mixing layer, we examined the process of generating the random small eddies in the flow. The fine eddies were first detected in the core of the streamwise vortices at the point where the merging of the spanwise structures occurred [Ref. VII-1, 2, 3, 4, 5 and 6]. In other words, the vortex merging not only transferred the energy to the subharmonic range, but also shifted the energy to the high frequency end.

VIII: Sound Generation

A numerical code of the compressible plane mixing layer was used to study the production of sound waves from the flow. We concentrated specially on the Mach number range that the hydrodynamic wavelength is about the same as the acoustic wavelength. In these cases, the pressure field can be calculated from the shear layer to the acoustic far field [Ref. VIII-1]. The results show the radiation patterns, the Mach number dependence, the mechanism of sound production, etc. Many of the unknown aeroacoustic phenomena were revealed by this powerful numerical method.

Index of Publications

I. Control of 2-D Coherent Structures.

1. "Vortex Merging in an Unforced Mixing Layer", with Huang, L.S., Bulletin of the American Physical Society, Vol. 26, p. 1267, 1981.

2. "Local and Global Dynamics of the Free Shear Layers", Numerical and Physical Aspects of Aerodynamic Flows, pp. 521-533, Springer/Berlin, 1982.

3. "Subharmonics and Vortex Merging in Mixing Layers", with Huang, L.S., Journal of Fluid Mechanics, Vol. 119, pp. 443-473, 1982.

4. "The Mixing Layer: An Example of Quasi Two-dimensional Turbulence", with Browand, F.K., Journal de Mecanique Theorique et Appliquee, pp. 99-120. 1983.

5. "Perturbed Free Shear Layers", with Huerre, P., Ann. Rev. of Fluid Mech., Vol. 16, pp. 365-424, 1984.

6. "Forced Unbounded Shear Flows", with Browand, F.K., Nuclear Physics B, Vol. suppl. 2, pp. 139-158, 1987.

II. Instrumentation.

1. "Response of Split Film Probe under Electrical Perturbations", Review of Scientific Instruments, Vol. 53, pp. 1240-1245, 1982.

III. Lock-on of Wake Flow.

1. "Lock-on and Instability in a Flat Plate Wake", with Masselin, M., AIAA Paper No. 85-0571, 1985.

IV. Subharmonic Resonance.

1. "A Free Shear Layer Forced by Fundamental and Subharmonic", with Zhang, Y.Q., Monkewitz, P., Laminar Turbulent Transition, ed. by V.V Kozlov, pp. 385-395, 1985.

V. Streamwise Vortices.

1. "On the 3-D Structures of a Mixing Layer", with Huang, L.S., Bulletin of the American Physical Society, bol. 28, p. 1380, 1983.

2. "Development of Free Shear Layers", with Huang, L.S., Turbulence and Chaotic Phenomena in Fluids, Pub. North Holland, ed. Tatsumi, T., pp. 327-332, 1983.

3. "Evolution of Streamwise Vortices in Mixing Layers", with Zohar, Y., Moser, R., and Rogers, M.M., Bulletin of the American Physical Society, Vol. 33, p. 2255, 1988.

4. "Evolution of Mixing Layers with a Spanwise Thickness Variation", with Rogers, M.M., Zohar, Y. and Moser, R.D., Bulletin of the American Physical Society, Vol. 33, p. 2274, 1988.

VI. Phase Decorrelation.

1. "Phase Decorrelation of Coherent Structures in Mixing Layers", with Zohar, Y. and Foss, J., Bulletin of the American Physical Society, Vol. 32, p. 2048. 1987.

2. "Phase Decorrelation of Coherent Structures", with Zohar, Y. and Foss, J., in preparation, 1989.

VII. Mixing Transition.

1. "Fine Scale Transition in Free Shear Layers", with Huang, L.S., and Hsaio, F.B., Bulletin of the American Physical Society, Vol. 30, p. 1744, 1985.

2. "Mixing Processes in Free Shear Layers", Invited Paper, AIAA Paper No. 86-0234, 1986.

3. "Evolution of Coherent Structures", Conference on Turbulence Structures in Free Shear Flows and Their Detection by Proper Orthogonal Decompositon, Newport, Rhode Island, 1988.

4. "Transiton from Deterministic Structures into Random Eddies", with Zohar, Y., Foss, J. and Huang, L.S., Second European Turbulence Conference, Berlin, Germany, 1988.

5. "Small Scale Transition in a Plane Mixing Layer", with Huang, L.S., submitted to Journal of Fluid Mechanics, 1989.

VIII. Sound Generation.

1. "Sound Generation by Supersonic Shear Layers", with Lele, S.K., Bulletin of the American Physical Society, Vol. 33, p. 2255, 1988.

Growth of Turbulent Regions in Unstable Boundary Layers
(Task 3)

Principal Investigator: Ron Blackwelder

Summary of Work Accomplished

I. Inflectional Velocity Profiles and a Turbulent Production Mechanism

The major discovery found during this contract was that turbulence production within transitional and turbulent boundary layers is associated with instantaneous inflectional velocity profiles. This is a different and more distinct mechanism than has been proposed before and suggests some new methods of controlling the turbulence production as discussed by Blackwelder(1988) and Swearingen and Blackwelder(1989).

Essentially this new idea for turbulence production evolves around the instability of a shear layer with an inflectional velocity profile. It has been known since the time of Rayleigh that these profiles are unstable to small disturbances and have an extremely rapid growth rate. The growth of a disturbance is so large that laminar wakes and jets are almost impossible to obtain experimentally. Instantaneous velocity profiles obtained in transitional and turbulent boundary layer during the course of this research revealed that these flows have inflection points also, although they do not occur continuously in time nor everywhere in space. Examples of these profiles and details of the production mechanism are given in Blackwelder and Swearingen(1989) attached as appendix A. They show that these profiles exist for sufficiently long periods of time that they can be considered as quasi-stationary and hence the results from steady state stability theory are applicable. They also show that the profiles occur at distances sufficiently removed from the wall that the viscous effects can be ignored.

One of the more surprising aspects of this mechanism is that inflectional profiles occur in both the normal and spanwise directions in transitional and turbulent layers. This is documented in figures 7 and 8 of Appendix A for a transitional layer on a curved surface and in figures 10 and 11 for the turbulent case. Heretofore, the spanwise direction has been neglected in the mechanisms for turbulent production; however these new results suggest that the local inflectional regions should be important and must be incorporated into any successful theory and model. The spanwise structure is especially important in attempting to explain the success of riblets in drag reduction; i.e. the riblets may act to slow the streamwise vortices and thus reduce the inflectional aspect of the velocity profile which in turn would reduce the production of turbulence.

II. Large Amplitude Laminar Disturbances

Another phase of this research during the last seven years has been to study the breakdown of a growing laminar disturbance into a turbulent patch of fluid. The earlier work of Blackwelder et al.(1984) and Tso et al.(1984) concentrated upon examining the initial conditions of a small perturbation within a laminar boundary layer. The importance of the spatial structure of the initial disturbance was examined by using various hole diameters and non-circular shaped holes for the injection of the minute disturbance. It was found when the initial disturbance is a pulse, that growing wave packets were produced only for the smallest diameter circular holes; e.g. 0.1 mm in diameter. Larger holes and non-circular holes tended to produce a different disturbance that broke down into turbulence much earlier. In all cases the initial break down into turbulence occurred at about $y = 0.2\delta$ and appeared upstream of the breakdown at $y = 1.1\delta$ observed by Gaster and Grant(Proc. Roy. Soc. Lond. A347, 1975). After the turbulent regions had a chance to develop downstream, a classical turbulent spot was observed in

turbulence occurred at about $y = 0.2\delta$ and appeared upstream of the breakdown at $y = 1.1\delta$ observed by Gaster and Grant(Proc. Roy. Soc. Lond. A347, 1975). After the turbulent regions had a chance to develop downstream, a classical turbulent spot was observed in all cases.

The temporal aspects of the initial disturbances were studied by Tso and Blackwelder(1985) by comparing the pulse disturbance described above with a tone burst consisting of 4 cycles of a sinusoidal wave. At low amplitudes, the tone burst disturbance evolved into a Gaster type wave packet downstream. With a large amplitude, a classical turbulent spot was generated almost immediately. At intermediate amplitudes, a wave packet was observed initially downstream. However another perturbation was also observed which had a larger lengthy scale and faster propagation velocity. Further downstream, this larger disturbance grew to greater amplitude and moved ahead of the wave packet which was travelling at the speed of the Tollmien-Schlichting waves. This larger disturbance broke down into a classical turbulent spot and the wave packet remained behind it as seen by Wygnanski et al.(JFM,92, 505, 1979). This observation explains the existence of the trailing wave packets and illustrates why the packets are correlated with the generation mechanism as observed by Wygnanski et al. Tso et al.(1988) have continued to investigate the breakdown of these different type of disturbances into turbulent spots.

III. Overhang Region of a Turbulent Spot

It had been conjectured in the literature that the overhang (of nose) region of a turbulent spot is very important in the growth of the spot because it contains turbulent fluctuations that could disturb the unstable laminar boundary lying beneath it. These disturbances would then be amplified by an instability mechanism in the laminar region, grow and breakdown into turbulence. The shape of the overhang region and other aspects of the leading edge of the spot were investigated by Gutmark and Blackwelder(1987). The distance that the overhang extended upstream from the turbulent interface at the wall increased continuously as the spot grew downstream. It appeared that the extent of the overhang was a function of the previous history of the spot and not necessarily a function of the Reynolds number.

The mixing characteristics within the turbulent spot were examined by Swearingen and Blackwelder(1985) by generating a fully developed spot and passing it over a heated wall region. The old turbulence was colder fluid and the newer turbulence generated in the vicinity of the wall was warm. The results indicated that the new turbulence is very dynamic and immediately dominates the flow field. However a sharp demarcation between the heated and non-heated regions could not be obtained due to the conductivity of the plate; thus this line of research was not continued.

Indes of Publications

Tso, J., Chang, S.-I., and Blackwelder, R.F., "On the Breakdown of Wave Packets in a Flat Plate Boundary Layer Flow," submitted for publication.

Blackwelder, R.F. and Swearingen, J.D., "The Role of Inflectional Velocity Profiles in Wall Bounded Flows," Near-Wall Turbulence, Ed. S.J. Kline, Hemisphere Pub. Corp., 1989.

Tso, J., Blackwelder, R.F., and Chang, S.-I., "On the Breakdown Mechanism of Three-Dimensional Disturbances in a Laminar Boundary Layer," Bull. Am. Phy. Soc., 33, 2226, 1988.

Blackwelder, R.F. "Coherent Structures Associated with Turbulent Transport," Transport Phenomena in Turbulent Flows, Ed. M. Hirata and N. Kasagi, p 69, Hemisphere Pub. Corp., 1988.

Gutmark E. and Blackwelder, R.F., "On the Structure of a Turbulent Spot in a Heated Laminar Boundary Layer," Experiments in Fluids, 5, 217, 1987.

Tso, J. and Blackwelder, R.F., "Transition of Wave Packets in a Flat Plate Laminar Boundary Layer," Bull. Am. Phy. Soc., 30, 1748, 1985

Swearingen, J.D. and Blackwelder, R.F., "Mixing Characteristics of a Turbulent Spot Passed over a Stepwise Discontinuity in Wall Temperature," Bull. Am. Phy. Soc., 30, 1751, 1985.

Blackwelder, R.F., Tso, J. and Kaplan, R.E., "Nonlinear Development of a Wave Packet in a Flat Plate Laminar Boundary Layer Flow," Bull. Am. Phy. Soc., 29, 1555, 1984

Tso, J., Blackwelder, R.F. and Kaplan, R.E., "Development of Pulse Disturbances from a Slit in a Flat Plate Laminar Boundary Layer," Bull. Am. Phy. Soc., 29, 1555, 1984.

The Role of Inflectional Velocity Profiles in Wall Bounded Flows*

by

Ron F. Blackwelder
University of Southern California
Los Angeles, California 90089-1191

and

Jerry D. Swearingen
Naval Research Laboratory
Washington, D. C. 20375-5000

INTRODUCTION

Much of the research on turbulent boundary layer during the past twenty years has concentrated on the coherent eddies that control the flow field. The large scale structure of the outer flow field dominates the flow features there and contols the entrainment of irrotational fluid into the turbulent regions. Near the wall the flow field is dominated by a series of events, collectively called the bursting phenomenon, that are responsible for the turbulence production and the drag. This series of events consists of counter-rotating streamwise vortices, low speed streaks of fluid, lift up of that fluid off the wall, an oscillation of the lifted low speed streak and the rapid growth of that oscillation and its break down into turbulence. This sequence has been described in detail by Kline et al. (1967), Willmarth (1975), Cantwell (1981) and others. The main thrust of the present work is to examine the oscillation stage and suggest a mechanism by which this occurs.

STABILITY THEORY FOR INFLECTIONAL VELOCITY PROFILES

One of the earliest successes in stability theory was due to Rayleigh (1880) who showed that inflectional velocity profiles in an inviscid fluid are unstable to small disturbances. Viscosity has only a damping influence in these flow fields as discussed by Lin (1955). Michalke (1965) analysed the hyperbolic tangent profile for a mean parallel flow field given by

$$U(\xi) = \frac{U_0}{2} \cdot [\tanh(\xi/\Delta)]$$

where U_0 is the maximum velocity difference across the shear layer and 2Δ is its vorticity thickness as illustrated in figure 1. He assumed a spatially growing two dimensional disturbance in the form of a travelling wave given by

$$u'(x,\xi,t) = \hat{u}(\xi) e^{i(\alpha x - \omega t)}$$
$$v'(x,\xi,t) = \hat{v}(\xi) e^{i(\alpha x - \omega t)}$$

α is the complex wave number, $\alpha = \alpha_r + i\alpha_i$, and ω is a real frequency where x and ξ are the streamwise and cross stream coordinates, u' and v' are the respective velocity perturbation. His results yielded a broad range of growing harmonic disturbances with the most amplified wave number being $\alpha_r\Delta = 0.40$. The corresponding wavelength is $\lambda_x = 15.7\Delta$ which is long compared to the shear layer thickness.

---

*From Near-Wall Turbulence, a Symposium held May 16-20, 1988 in Dubrovnik, Yugoslavia published by Hemisphere Pub. Corp.

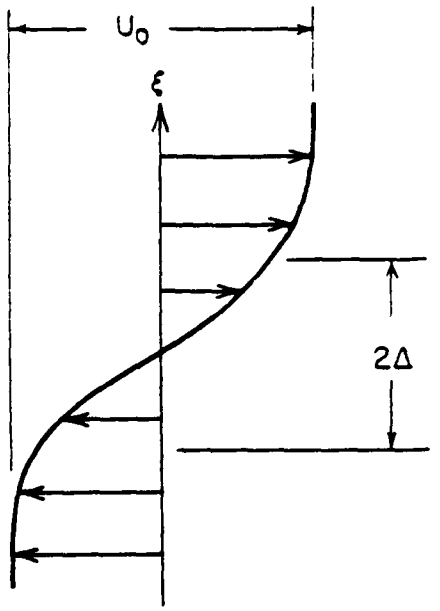

Fig. 1. Sketch of an inviscidly unstable velocity profile in the ξ direction.

More surprising however is the growth rate of these disturbances, α_i. Michalke's analysis shows that the disturbances grow like $e^{\alpha_i x}$ where the maximum growth rate was found to be $\alpha_i\Delta = -0.23$. Thus while the wavelike disturbance travels one wavelength downstream, $x-x_0 = \lambda_x$, it is amplified by a factor of 36 and its energy increases more than 1000 fold! For comparison, the maximum amplification of the most unstable Tollmien-Schlichting wave is typically 1.1 (i.e. they experience a 10% increase in amplitude) during a journey of one wave length downstream because its growth rate is an order of magnitude smaller. Hence disturbances associated with inviscid inflectional velocity profiles are amplified much more than those associated with viscous instabilities. In some transitional flow fields, the initial viscous instability amplifies an initial disturbance in a manner that produces an inflectional profile as discussed by Blackwelder (1983). This opens the door to another type of instability, usually called a secondary or higher order instability. If the secondary instability is an inflectional type, the disturbances will grow much faster than the initial disturbance and will dominate the transition process.

One of the more interesting characteristics of the inviscid instability is that its amplification is strongly dependent upon the shear rate of the inflectional profile. To illustrate this, note that the maximum amplification over the distance x_2-x_1 is given by

$$e^{0.23\,(x_2-x_1)/\Delta} \qquad (1$$

Thus the smaller the length scale Δ, the larger the growth over the same distance. Figure 1 shows that Δ is inversely proportional to the maximum shear of the profile, i.e.

$$\left.\frac{\partial U}{\partial \xi}\right|_m = \frac{U_0}{2\Delta}$$

Eliminating Δ between these two expressions yields a growth of

$$\frac{.46}{U_o}\frac{\partial U}{\partial \xi}\bigg|_m (x_2-x_1) \qquad (2$$

Consequently the maximum amplification experienced by a disturbance over the distance x_2-x_1 downstream depends strongly on the mean shear at the point of inflection.

The above arguments following Michalke's analysis have been for a steady two-dimensional inflectional profile in a parallel flow. To apply these arguments in a transitional or turbulent flow, the restrictions imposed by these assumptions must be addressed. The effects of non-parallel flow have been examined by Gaster et al. (1985). They found that when the local value of the mean flow was used for the stability calculations, the theory accurately predicted the measured fluctuations even though the flow was nonlinear. Greenspan and Benney(1963) have studied the effects of an unsteady mean flow by allowing the thickness, Δ, to vary sinusoidally with time. The forcing period was much larger than the time scale of the instability. They found that the unsteadiness increased the growth rates so that the energy of the disturbance increased by 10,000 over one wavelength!

Another limitation of the above analysis is that it pertains only to unbounded flow domains. However Huerre (1983) has considered the same inflectional velocity profile confined by two side walls located at $\xi = \pm d$. He assumed the normal velocity on the walls was zero but allowed a slip condition to occur to simplify the analysis. He found that if $d > 1.2\Delta$, the linear stability characteristics were similar to the inviscid theory and the wall had little effect on the growth of the disturbances.

The two-dimensionality of the mean flow has not yet been addressed and is still an open question. However, Nishioka et al. (1980) applied the inviscid two-dimensional theory to an inflectional U(y) velocity profile in a transitional channel flow. The instantaneous velocity profile was formed by the Tollmien-Schlichting waves and was strongly three-dimensional. Experimentally they observed that a secondary instability appeared at the location of the inflection point. To examine this in more detail, they applied the two-dimensional inviscid calculation discussed above and found that it predicted the measured wavelength and eigenfunction. The measured growth factor was approximately 60% of the theoretical value. Similar results have been observed in transitional boundary layers on flat and concave plates. The reduced growth rate may be due to the spreading of energy into the third dimension which is not accounted for in the two-dimensional theory. This effect indicates that the disturbance would be amplified by a factor of 9 after travelling one wavelength downstream rather than by 36 mentioned earlier. The net result is that even though the growth rate may be reduced by the three-dimensionality, it is still very large.

GÖRTLER INSTABILITY ON A CONCAVE WALL

The Görtler instability is one member of a class of centrifugal instabilities including the Taylor, Dean, etc. instabilities. These instabilities arise as a result of an imbalance between a centrifugal force imposed on the fluid and the restoring pressure force. The Görtler instability develops within a boundary layer developing on a concave wall. The curvature of the wall imposes a centrifugal force within the fluid that acts to displace fluid particles toward the wall. The pressure force acts to restore the particles to their original position. This class of instabilites is inviscid in nature and the viscosity only acts to inhibit the motion, i.e. provides a damping force, just as in the inflectional profile instabilities. Therefore if the centrifugal force is smaller than the pressure force, the flow is stable. However if the centrifugal force sufficiently exceeds the pressure force such that the viscosity can no longer damp the motion, the flow field is unstable and small disturbances will be amplified.

Görtler(1939) first analysed this problem using temporal stability theory and found that the governing parameter for this flow was

$$G\ddot{o} = \frac{\theta U_\infty}{\nu}\sqrt{\frac{\theta}{R}} \qquad (3$$

This dimensionless number is known today as the Görtler number. If it exceeds a critical value of the order of unity, the flow is unstable and develops counter-rotating streamwise vortices lying within the boundary layer. These vortices are periodic in the spanwise direction and are characterized by a spanwise wave length λ_z. Hall (1983) has shown that for vortices with wavelengths λ_z comparable to the boundary layer thickness, the growth of the boundary layer cannot be neglected in the analysis. Consequently a unique neutral stability curve does not exist but rather depends upon the history of the boundary layer. Nevertheless, Hall found that each neutral stability curve had a minimum at $G\ddot{o} \sim 1.5$.

In a spatial analysis of the Görtler instability in a parallel flow, Smith (1955) assumed the disturbances on a concave wall grew by the factor $e^{\beta(x_2-x_1)}$ as they travelled downstream from x_1 to x_2. β is the growth rate and varies slowly in the downstream distance. As the fluid moves downstream from the leading edge, the disturbances are initially damped, i.e. $\beta < 0$. They crossed the neutral stability curve at $\beta = 0$ and are unstable, i.e. $\beta > 0$, further downstream. To compare this growth rate with the inviscid one, β must be determined. Liepmann (1945) has shown that Görtler instability transitions to turbulence when $G\ddot{o} = 9$. The nominal value of amplification rate slightly before transition, i.e. $G\ddot{o} = 7$, is $\beta\theta Re_\theta \sim 3$ according to Smith. For this value of the Görtler number, Re_θ ranges from 230 reported by Bippes (1972) to 360 from Swearingen and Blackwelder (1987). For $Re_\theta = 300$ and with the boundary layer thickness, δ, equal to 7.5θ as in a Blasius layer, the amplification becomes $e^{0.075\,(x_2-x_1)/\delta}$. Thus the streamwise vortical disturbance will double its amplitude after travelling 10δ downstream. For comparison, the most unstable Tollmien-Schlichting wave at $Re_\theta = 300$ has a wavelength of 8δ and an amplification factor of $e^{0.06(x_2-x_1)/\delta}$. These waves are amplified approximately 80% after travelling 10δ downstream. Hence at this Reynolds number, the Görtler instability has a slightly greater amplification than Tollmien-Schlichting waves. The conclusion is that the growth rates in both boundary layer flows are at least an order of magnitude less than that of the inflectional profile instability discussed earlier

THE BREAKDOWN OF GÖRTLER VORTICES

The above linear theory only describes the initial growth of a small disturbance on a concave wall. Like most linear theories, it can say nothing about the later growth stages and breakdown of the perturbation. In a visual study of the vortices on a curved plate Bippes (1972) has shown that the perturbation velocity profiles agreed well with the computed eigenfunctions and the growth rates were comparable to the values given by the linear theory. He also found that the disturbances grew to an amplitude of a few percent of the streamwise mean velocity while maintaining their streamwise vortical structure. However, after a limited domain of linear growth, the flow field developed a strong oscillatory motion before breaking down into turbulence.

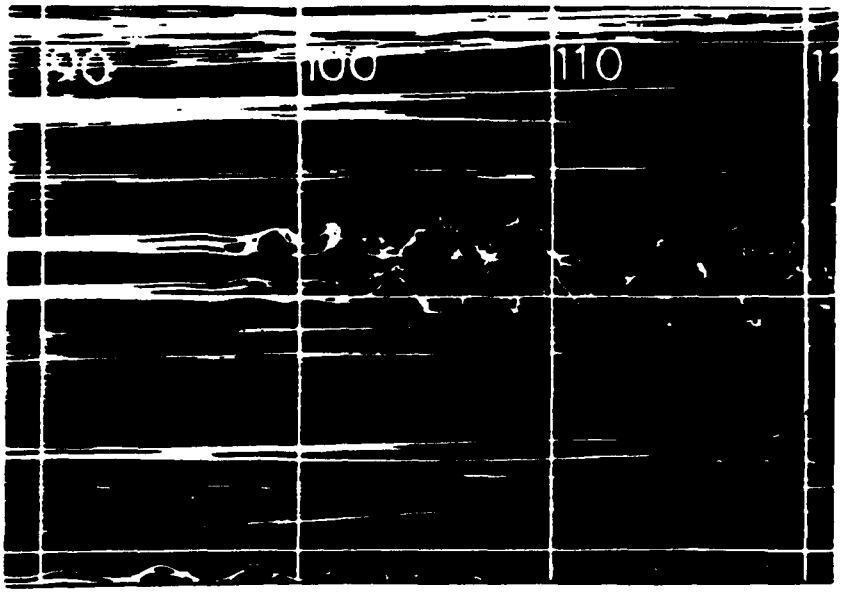

Fig. 2. Instantaneous visualizations of the Görtler instability and transition on a concave wall. The concentrated smoke marks the low speed streaks and the sinuous motion is a result of the inflectional instability.

This aspect of the motion was considered to be important in the transition process because it represented a shift from a primary to a secondary instability in the flow. Since similar observations have been made in the wall region of turbulent flows (see below), an experiment was set up to measure the velocity components in more detail to study this phenomenon. The specially designed wind tunnel used for this experiment had a curved test section with a cross sectional area of 15 x 120 cm. A boundary layer was developed on the concave wall having a radius of curvature of R = 3.2m with a free stream velocity of 5.0 m/sec. A smoke wire was used to visualize the flow field. The streamwise velocity was measured with rakes of hot-wires aligned in the spanwise and normal directions. Thus the U(z,t) and U(y,t) profiles could be measured instantaneously. The signals were digitized and stored on disc for later processing. Further details of the experimental arrangement may be found in Swearingen and Blackwelder (1987).

At a freestream velocity of 5 m/sec, the critical Görtler number occurred at approximately 10 cm downstream of the leading edge of the curved plate. When the smoke wire was placed into the lower regions of the boundary layer upstream, i.e. at y = 0.25δ, and x = 20 cm, the resulting flow downstream appeared as in figure 2. By the time the smoke was convected downstream, it had also been coagulated into elongated regions as seen in the photo. Swearingen and Blackwelder(1987) showed that the regions of strong smoke concentrations seen in the figure are also regions of low streamwise velocity. They also showed that the ensuing dynamics were concentrated around and directly related to the low speed regions.

A sketch of the streamwise vortices and the low speed regions is shown in figure 3. The initial instability produces the counter-rotating streamwise vortices with two vortices per spanwise wavelength. The strength of these vortices is quite small. To illustrate this, consider a mean parallel flow U(y) with a disturbance field u such that the total velocity is

$$\begin{aligned} u(x,y,z) &= U(y) + u'(x,y,z) \\ v(x,y,z) &= \quad\;\; v'(x,y,z)/Re \\ w(x,y,z) &= \quad\;\; w'(x,y,z)/Re \end{aligned} \qquad (4$$

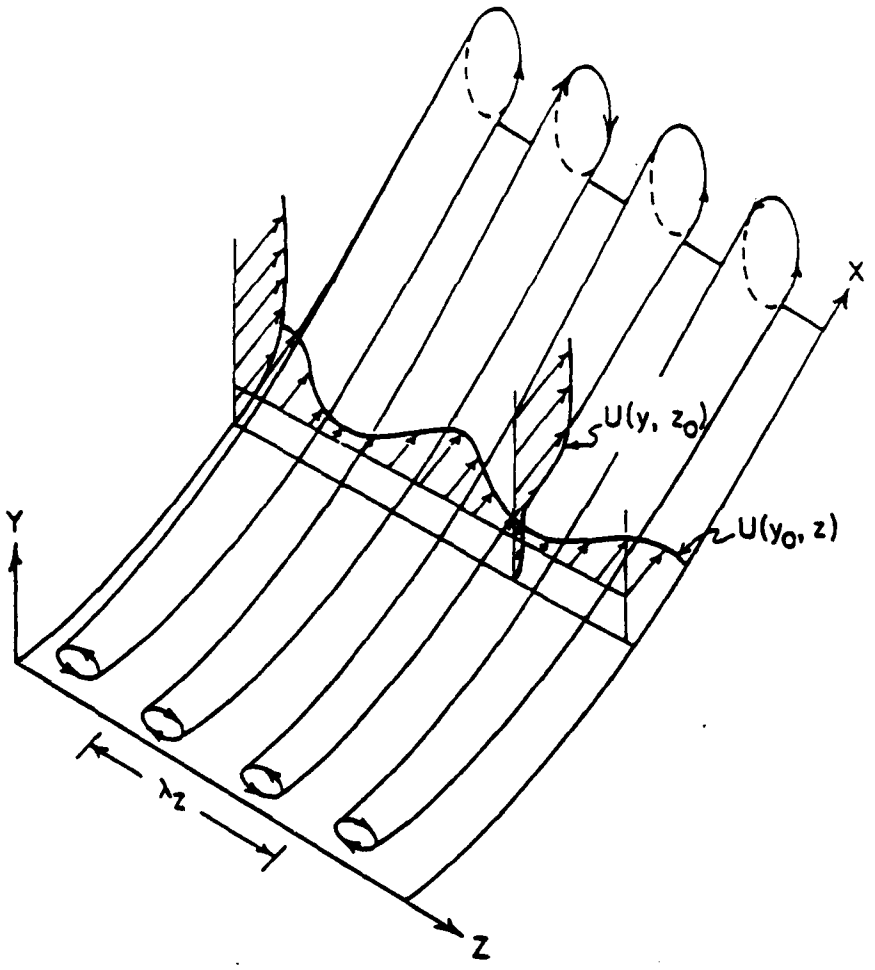

Fig. 3. The streamwise vortex system downstream of the critical Görtler number. The streamwise scale is compressed with respect to the other axes.

where Re is the Reynolds number. This scaling leaves u', v', and w' of the same order as suggested by Diprima and Stuart (1972) and verified by Floryan and Saric (1982). When the vorticity components are obtained from these equations, it is easily seen that the disturbance streamwise vorticity ω_x is smaller than both ω_y and ω_z by the factor Re^{-1}. Hence even though the flow field is generally described as a laminar boundary layer with embedded growing streamwise vortices, they contain only small amounts of streamwise vorticity.

The above illustration indicates that the phase of coherent eddies is much more important than the amplitude of their velocity or vorticity fields. It also suggests that detection of coherent structures should not be based on amplitude alone without considering phase information also. In the Görtler vortex case, the vortices do generate large vertical disturbances, namely $\omega_y = \frac{\partial U}{\partial z}$ and $\omega_z = \frac{\partial U}{\partial y}$. But any detection scheme based on amplitude alone would probably fail to discern the underlying eddy structure, namely the streamwise vortices. Of course the reason the ω_x vortices are so effective is that they exist in a region of strong mean shear, $\frac{\partial U}{\partial y}$, and thus a very small ω_x rotation can produce large disturbances across the span.

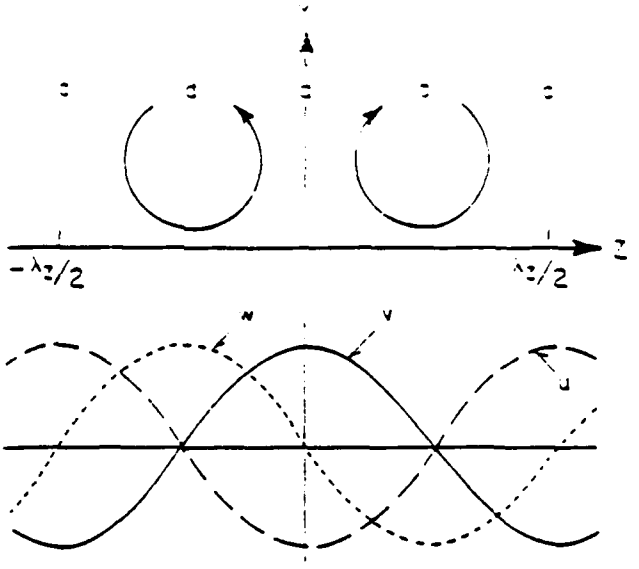

Fig. 4. Illustration of the relative phase of the disturbance velocity components at positions below the centers of the streamwise vortices. The velocity amplitudes depend on y and are not to scale.

Between the vortices in figure 3 are alternating regions of low and high speed fluid. These regions are a natural result of the counter-rotating vortices lying is a strong shear flow. The velocity field associated with the vortices has a normal velocity component with a relative maximum or minimum between the vortices at positions a and c respectively as seen in figure 4. Simultaneously the fluid lying below the centers of the vortices has a spanwise velocity component that alternates in sign with the vortices so that its motion is directed towards the region of positive normal velocity. The combined action of two vortices is to displace lower speed fluid originally near the wall into a region lying between the vortices shown at position a in figure 4. This creates the elongated low speed regions seen in figure 3. On the other hand, the higher speed fluid lying above the centerline of the vortices experiences a relative motion that forms concentrations of high speed fluid between alternate vortices at positions c in figure 4.

One of the principal results of this vortical motion and the unique aspect of the Görtler instability is that it creates inflectional velocity profiles in a flow field in which there were none before the disturbance started to grow. It is interesting to note that a spanwise inflectional profile will develop as soon as the vortices begin to grow. This is best illustrated by considering the usual velocity perturbations, i.e.

$$\begin{aligned} u'(x,y,z) &= -\hat{u}(y)\cos\alpha z\, e^{\beta x} \\ v'(x,y,z) &= \hat{v}(y)\cos\alpha z\, e^{\beta x} \\ w'(x,y,z) &= -\hat{w}(y)\sin\alpha z\, e^{\beta x} \end{aligned} \tag{5}$$

As soon as this disturbance begins to grow, there are inflection points in the u(z) profile at $\alpha z = \pm(n+\frac{1}{2})\pi$, $n = 0,1,2\ldots$ The strength of the strain rate at these points is

$$\left|\frac{\partial u}{\partial z}\right| = \alpha\hat{u}(y)\, e^{\beta x}$$

and it increases in magnitude with the growth of the instability. Note that the sign of the strain rate is not essential in the inviscid instability; only the absolute value is important. Later in the development of the flow, inflectional U(y) profiles develop as predicted and observed by several investigators. These inflectional profiles open the door to an inviscid instability as discussed above.

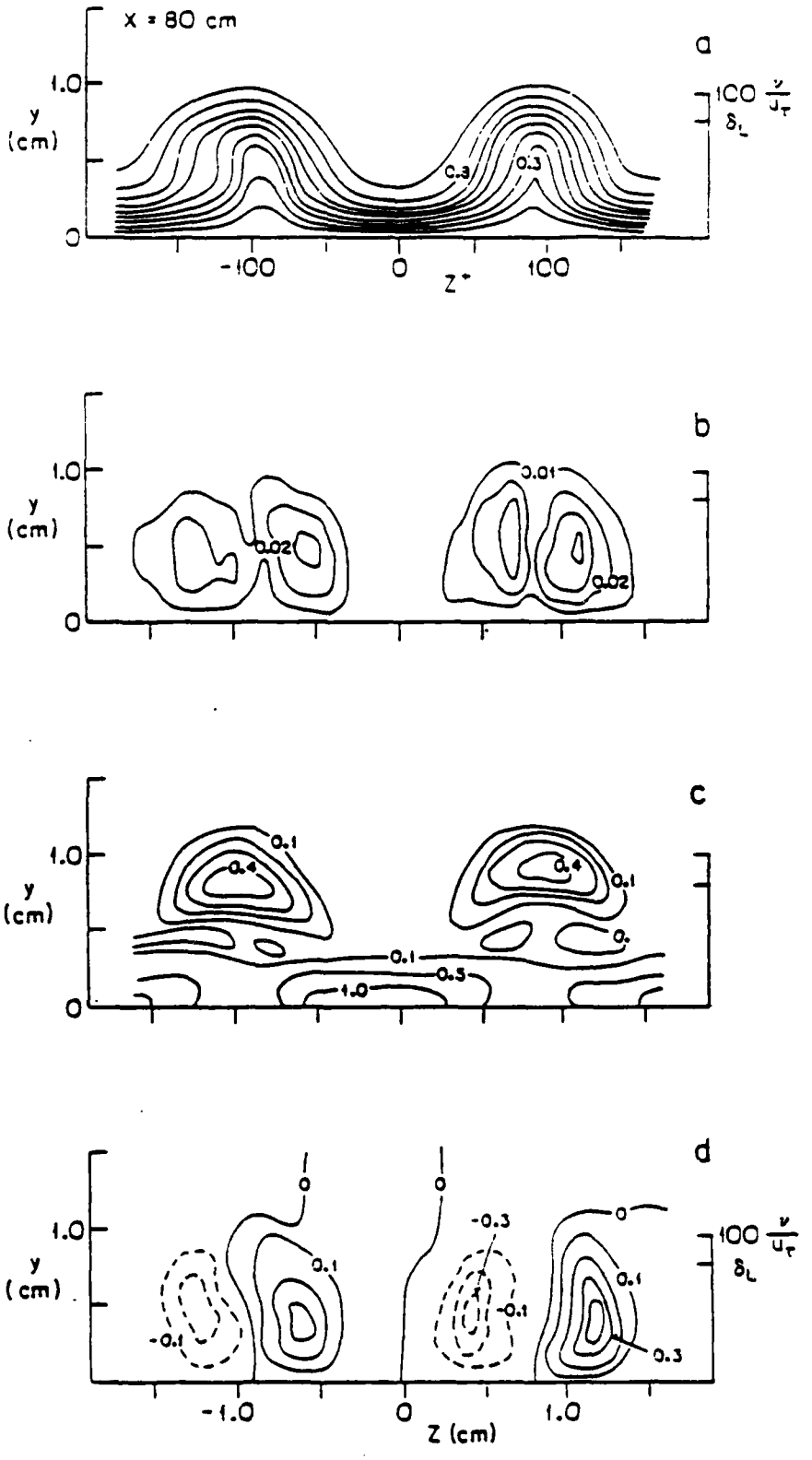

Fig. 5. From top to bottom are the iso-contours of a) the mean velocity, b) the rms velocity, c) the normal shear $\partial U/\partial y$ and d) the spanwise shear $\partial U/\partial z$. The data were taken at y = 80 cm and are normalized with the free stream velocity and the velocity gradient at the wall.

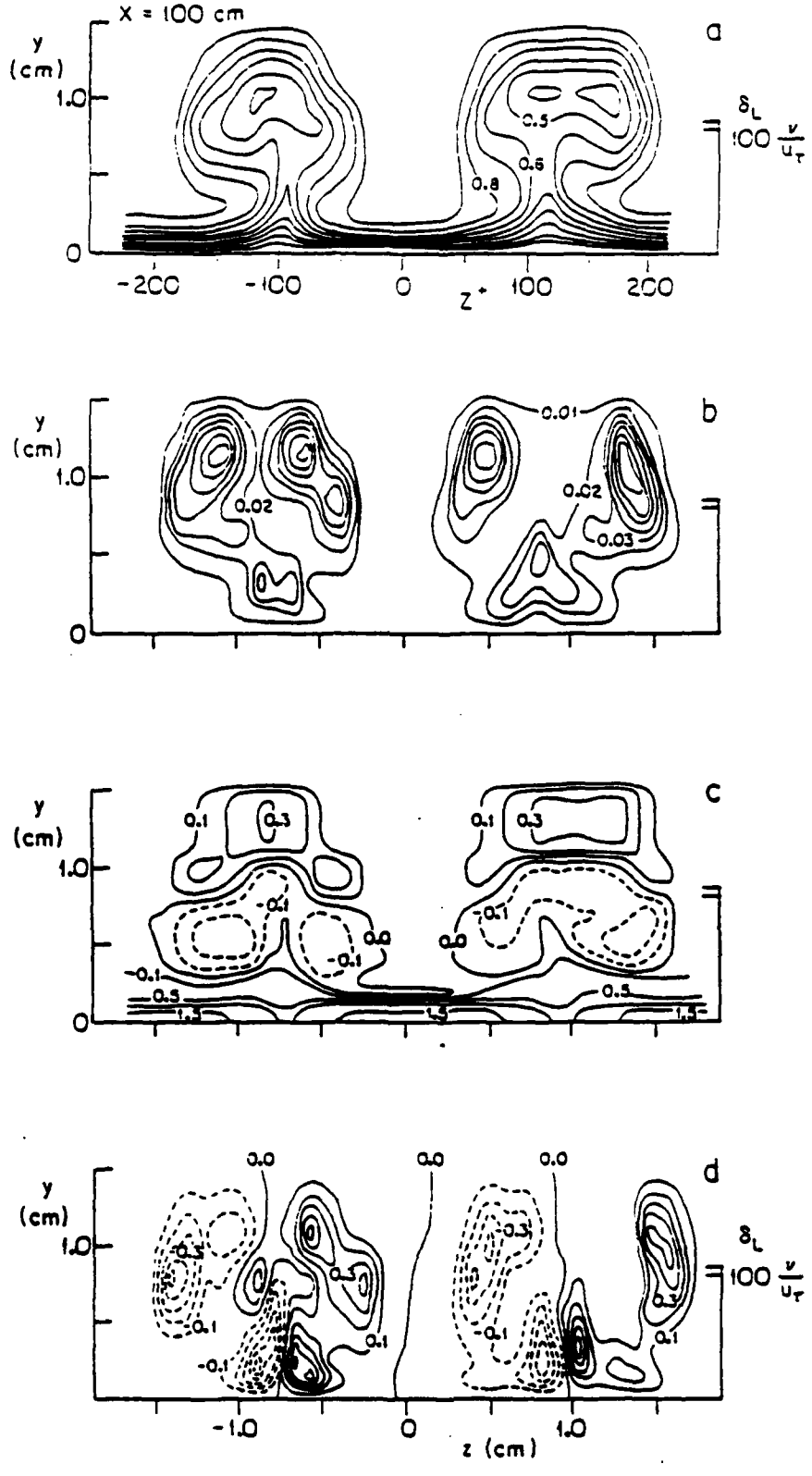

Fig. 6. Similar to figure 5 at x = 100 cm.

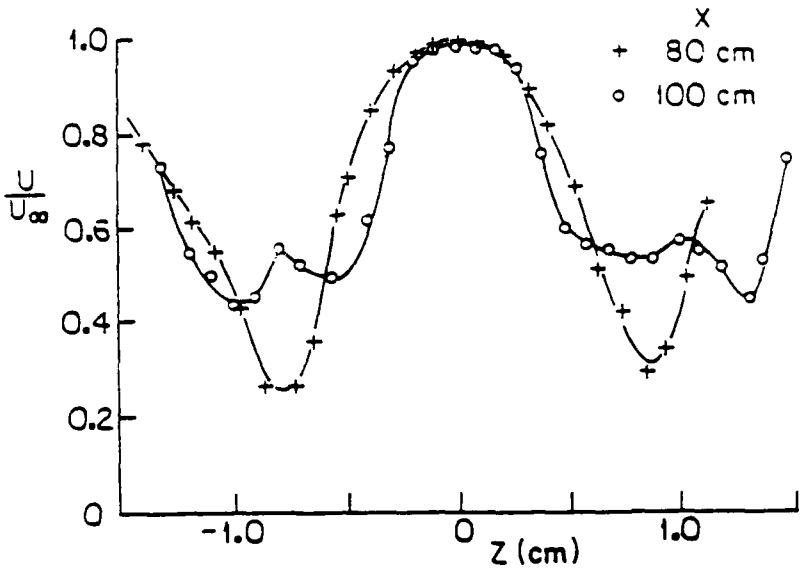

Fig. 7. Two examples of the spanwise velocity profile having inflection points and large shear.

local $\partial U/\partial z$ maxima occurs at the identical location of the maxima in the rms contours and their contour shapes are very similar (compare with figures 6b and 6d). Even the new local maximum near the wall at x=100cm in the fluctuation contours is also found in the iso-shear plot. Hence it it obvious that the velocity fluctuations are associated primarily with the spanwise shear rate, $\partial U/\partial z$.

Examples of the mean spanwise velocity profiles obtained at the y position near the maximum in the $\partial U/\partial z$ contours are shown in figure 7 for x = 80 and 100cm. The mean spanwise averaged velocity is approximately $0.7U_\infty$ in both cases and the maximum shear is typically 0.5 $\partial U/\partial y|_w$. To illustrate the stability theory predictions, the theoretical wavelength associated with these profiles should be $\lambda_z = 15.7\Delta$. From figure 7 at 100 cm the shear layer thickness is approximately 0.25cm. This yields $\lambda_z \sim 3.9$cm which compares favorably with the wavelength seen in figure 2.

Similar profiles in the normal direction are shown in figure 8 at four downstream locations. The inflection points are noted and it is easily seen that the inflections move rapidly away from the wall as the flow moves downstream. The velocity at the inflection points is typically $0.65U_\infty$.

WALL REGIONS OF BOUNDED TURBULENT SHEAR FLOWS

The wall region of bounded turbulent shear flows is dominated by the bursting process which is composed of a series of events similar to that described above for the Görtler problem. Namely there are streamwise vortices, elongated regions of low speed fluid called low speed streaks, lift-up and oscillation of these streaks and a rapid disintegration of the coherent motion followed by strong mixing.

The role of the streamwise vortices in the turbulent flow is less clear than in the Görtler case. Indeed, there is no generally accepted definition of such vortices found in the literature. Let us make the following definition:

> A vortex consists of a coherent vortical parcel of fluid such that the instantaneous streamlines in the plane perpendicular to the vortex lines are closed.

By the time the flow has reached 100cm downstream in the experiment, the velocity field was strongly nonlinear as evidenced by the variations in the measured streamwise velocity component. Figures 5 & 6 illustrate the iso-velocity contours measured over two wavelengths in the spanwise direction at two downstream locations, x = 80 and 100 cm. Two low speed regions at z ≅ -0.8 and +0.8cm are evidenced by the relative lower speed fluid lying at the elevated regions. The U(y) = 0.9 contour lies well beyond the nominal boundary layer thickness defined by $U(\delta_L) = 0.99U_\infty$. The growth of the low speed region has been quite large; the $U = 0.9U_\infty$ contour has been displaced outward from 1.25 to 1.75 δ_L where δ_L is the corresponding Blasius layer thickness at each location. Hence the disturbance has a large growth rate compared to the nominal laminar boundary layer. The displacement thickness at these locations was measured to be approximately $\delta^* = 0.7$cm compared with the Blasius value of $\delta^* = 0.28$cm. The corresponding higher speed regions at z = 0 and ±1.6cm have thinned the boundary layer considerably such that $\delta^* = 0.1$cm there. In these locations the shear is especially strong near the wall compared with the shear in the lower speed regions.

As noted earlier, the Görtler instability grows spatially downstream and has no temporal dependence. However oscillations do develop downstream as seen in figure 2 which indicate the presence of a secondary instability. The temporal fluctuations were measured and their iso-contours are given in figures 5b and 6b at the two locations. Note that the maximum at each position occurs on the sides of the low speed streak and not near the top. The maximum magnitude increases from roughly $0.03U_\infty$ to $0.08U_\infty$ bewteen 80 and 100 cm downstream. The total energy associated with the temporal oscillations is proportional to the square of the u′ values integrated over the y-z plane. Clearly this energy has increased by more than an order of magnitude.

It is also significant that the locii of the iso-contours have moved outward from the wall. The maximum at x = 80cm is at 0.5cm and the corresponding maximum at x = 100cm is at 1.15cm. The corresponding Blasius thickness, δ_L, has only increased from 0.78cm to 0.86cm. This outward movement corresponds to an average normal velocity greater than $0.03U_\infty$ which is more than an order of magnitude greater than the Blasius velocity normal to the plate.

Another important feature of figure 6b is that as the primary fluctuations have moved outward, a new local maximum has evolved in the wall region at x = 100cm. At 110cm downstream, this maximum was approximately $0.12U_\infty$ whereas the outer maximum had remained constant at $0.08U_\infty$. After 110cm, the entire layer became turbulent and the local maxima were no longer discernable.

The reason for the occurrence of two maximum rms values per wave length is apparent when the iso-shear contours are examined in figures 5cd and 6cd. The $\partial U/\partial y$ and $\partial U/\partial z$ gradient fields were calculated by fitting the averaged velocity data with a spline fit and then differentiating. They are normalized with the average gradient at the wall which was 1650 and 2300 sec^{-1} at x = 80 and 100cm respectively. The $\partial U/\partial y$ iso-shear contours are presented in figures 5c and 6c and the corresponding $\partial U/\partial z$ contours in 5d and 6d at the two streamwise locations. The normal shear $\partial U/\partial y$ has its maximum at the wall as expected, but also develops a strong local maxima above the low speed streak. This maxima moves outward as it travels downstream and is reduced slightly in magnitude. Distinct regions of negative shear are seen at x = 100cm due to the low speed fluid riding above higher velocity fluid as seen in figure 6a.

The spanwise shear rate, $\partial U/\partial z$, has a distinct minimum and maximum on both sides of the low speed streaks. Symmetry indicates the minimum and maximum must have the same magnitudes; however for these two streaks studied, the negative amplitude was always slightly less. The maximum magnitude of $\partial U/\partial z$ is comparable to that of $\partial U/\partial y$ at x = 80cm and exceeds $\partial U/\partial y$ at x = 100cm. The local maxima of the spanwise shear increases from 0.4 to $0.5u_\tau^2/\nu$ downstream in contrast to the decrease in $\partial U/\partial y$. The

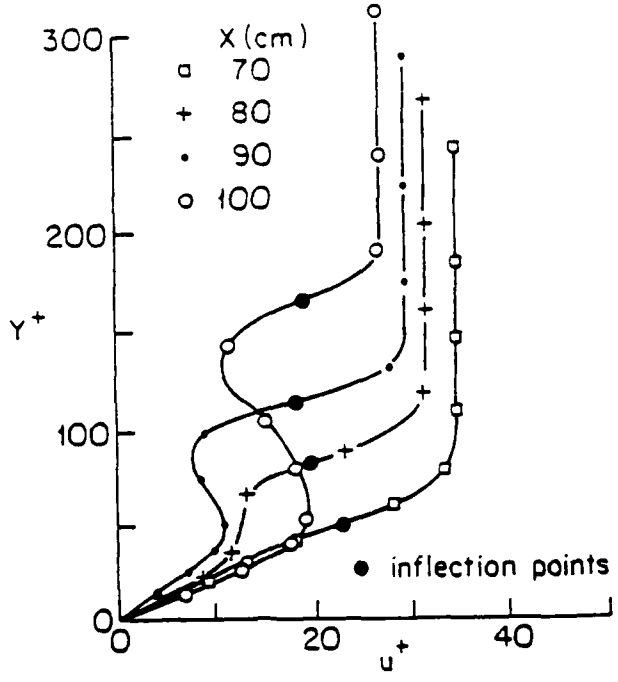

Fig. 8. **Evolution of the ∂U/∂y inflectional velocity profiles in the x direction along the centerline of a low speed region.**

This definition emphasizes the coherent aspects of the motion which are associated with and due to its phase and not necessarily due to its amplitude. Thus it includes the weak Görtler streamwise vortices, vortex rings, trailing wing tip vortices, etc., but excludes the mean vortex lines in a two-dimensional shear flow.

Evidence of such vortices in the wall region has been assumed by many authors, however very little quantiative ata exists supporting their existance. Most of the data that are available are visual results such as those of Kline et al. (1967) and Smith and Schwartz (1983). Both of these authors have used hydrogen bubbles to visualize the flow field and have shown that often the hydrogen bubbles are coagulated into a confined region with definite rotation perpendicular to its principal axis consistent with the above definition of a vortex. Smith and Schwartz speculated that the observed streamwise rotations were due to the legs of horseshoe type vortices. Acalar and Smith (1987ab) have set up two model laminar flow fields to study the vortical nature of the motion near a solid boundary. In the first, they studied the flow over a hemisphere and the second was the flow over lower speed fluid injected through a streamwise slit in the wall. In both cases they observed the periodic formation of repeatable horseshoe vortices. The structure was studied by placing the hydrogen bubbles at different positions and photographing the vortices at different times after their formation. Their visual results are very similar to photographs obtained in the turbulent wall region and suggest that similar vortices appear there also. Kim and Moin (1986) have observed similar type structures in their numerical data by tracing vortex lines. By examining regions of strong streamwise vorticity, they concluded that the associated vortex lines rarely remained parallel to the wall for distances greater than 100 ν/u_τ. This result is consistent with the above observations by Smith and Schwartz.

The conditionally averaged data of Blackwelder and Eckelmann (1979) and of Kim (1983) also support the idea that streamwise vortices exist in the wall region. Even though their results yielded symmetrical vortices, the symmetry was a result of the technique and does not imply that symmetrical pairs will occur. Guezennec et al. (1987) have shown that the vortices rarely appear in a symmetrical manner, but one vortex is usually much larger than the other. Obviously spanwise symmetry requires that the average streamwise vorticity be zero.

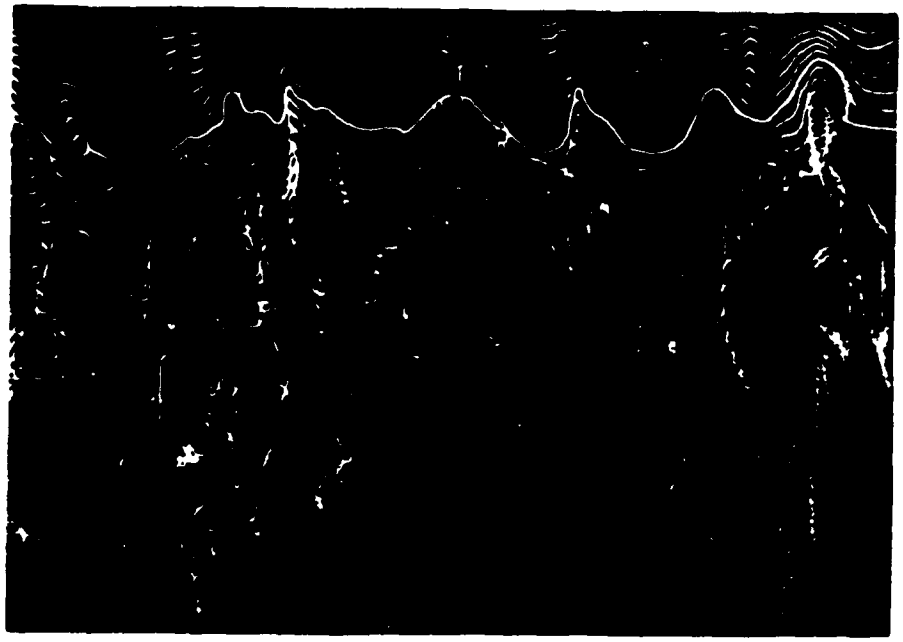

Fig. 9. Visualization of the low speed streaks and eddy structure in the wall region made visible by a hydrogen bubble wire at $y^+ = 12$.

The most ubiquitous structures of the wall layers are the low speed streak. They have a width of $20\nu/u_\tau$, an average spanwise spacing of $100\nu/u_\tau$, and have steamwise lengths up to and exceeding $1000\nu/u_\tau$. The low speed streaks are most readily observed by hydrogen bubbles as seen in figure 9. The hydrogen bubble wire is seen at the top left hand corner of the photograph and was pulsed at 40 Hz. The wire was at $y+ = 12$ and the mean flow velocity was 10 cm/sec. The low speed streaks are readily recognizable by the closeness of the bubble lines and the higher concentration of bubbles. The spanwise scale of the low speed regions is roughly $20\nu/u_\tau$. The spanwise scale of the higher speed fluid is much larger, typically about $60\nu/u_\tau$, so that the spanwise spacing between low speed streaks is typically $80\nu/u_\tau$. All of these dimensions are random variables and hence only average values can be used for the scales.

Since the pulsed line of bubbles is a time line, its x position downstream of the bubble wire is proportional to the Langrangian streamwise velocity component. A highlighted time line is shown in figure 9 to illustrate the U(z) velocity profile. Neglecting the difference between the Langrangian and Eulerian velocities for the moment, one can see that the U(z) profile has a strong variation across the field; its approximate minimum is $0.2U_\infty$ and its corresponding maximum is $0.8U_\infty$. Also of importance is the fact that due to this variation, there are points of inflection in the profile on both sides of the low speed streaks. These regions are possible sites for an inviscid inflectional instability as discussed earlier. In addition, the shear rate there is found to be extremely large, i.e. of the same order of magnitude as the shear rate at the wall which is u_τ^2/ν.

This phenomenon was studied in more detail in a turbulent boundary layer at $Re_\theta = 2200$ by using multiple hot-wire probes spanning the y and z directions. Since they are sensitive to the streamwise velocity, they measure the U(y) and U(z) profiles as seen in figure 10. The data from each sensor is plotted and the solid line is a spline fit of the data. The spline fit was differentiated to determine the locations of the inflection points which are denoted. A comparison of figure 9 and 10 indicates that the shear rates are slightly higher in the visualization results probably due to the finite resolution of the hot-wire sensors. Nevertheless, it is obvious that there are many inflection points in both U(y) and U(z) in the wall region.

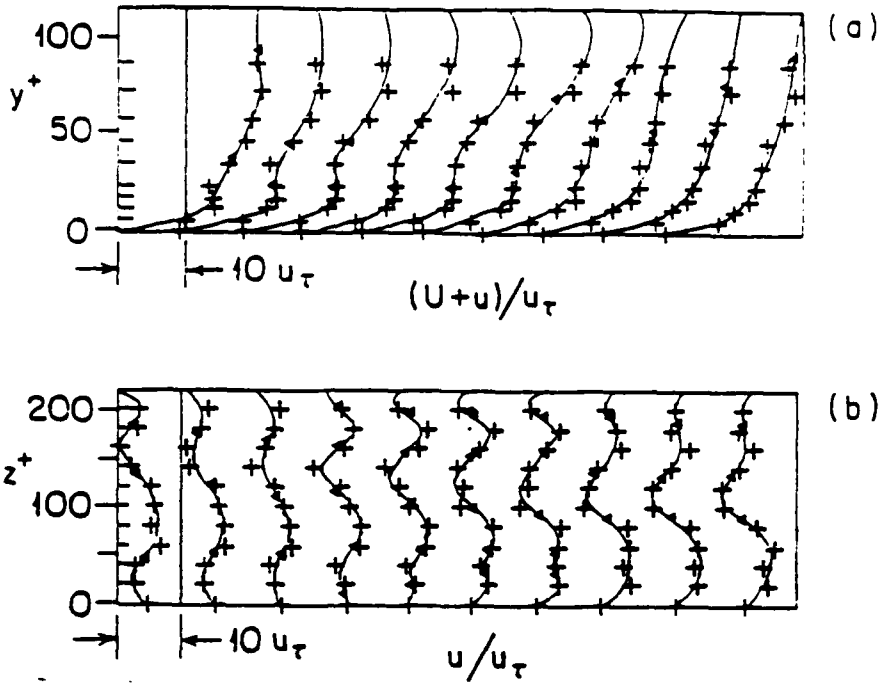

Fig. 10. Instantaneous turbulent boundary layer profiles from hot-wire sensors of the streamwise velocity component in the (a) normal and (b) span-wise directions. The data points are indicated by (+) and a spline fit yielded the lines. The points of inflection (◀) were obtained from the spline function. The time between profiles is $1.5\nu/u_\tau^2$ in (a) and $1.0\nu/u_\tau^2$ in (b).

Figure 11 gives another example of the ubiquitous nature of the inflectional profiles. These results were obtained from the numerical simulation of a turbulent channel flow at $Re_\theta = 200$. The data were searched for points of inflection which are denoted on the figure. Comparing figures 10 and 11 suggests that the lower Reynolds number channel flow has more inflection points; however, this is most probably an illusion due to different techniques used for the two data sets. It is quite evident that both the experimental and numerical data indicate that points of inflection are very evident in both the U(y) and U(z) data.

A comparison of figures 11b and 11c indicate that inflection points are much more predominate in the wall region at $y^+ = 15$ than in the logarithmic region at $y^+ = 66$. This agrees with the earlier idea that the low speed streaks are concomitant with inflectional profiles. Since the low speed streaks do not extend outward beyond $y^+ \sim 25$, one expects that fewer inflection points will be observed above that level.

In addition to the inflectional character of the velocity, several other conditions are necessary before the simple stability anayisis can be applied. First the flow should be steady; i.e. the changes in time in the base flow must have a much longer time scale that the time scale of the instability. Smith and Metzler (1983) have measured the persistence of the low speed streaks and find that they have an average life time of $480\nu/u_\tau^2$ with some streaks persisting up to $2580\nu/u_\tau^2$. These values are much longer than the time scale of the instability which is of the order ν/u_τ^2. Thus, a quasi-steady

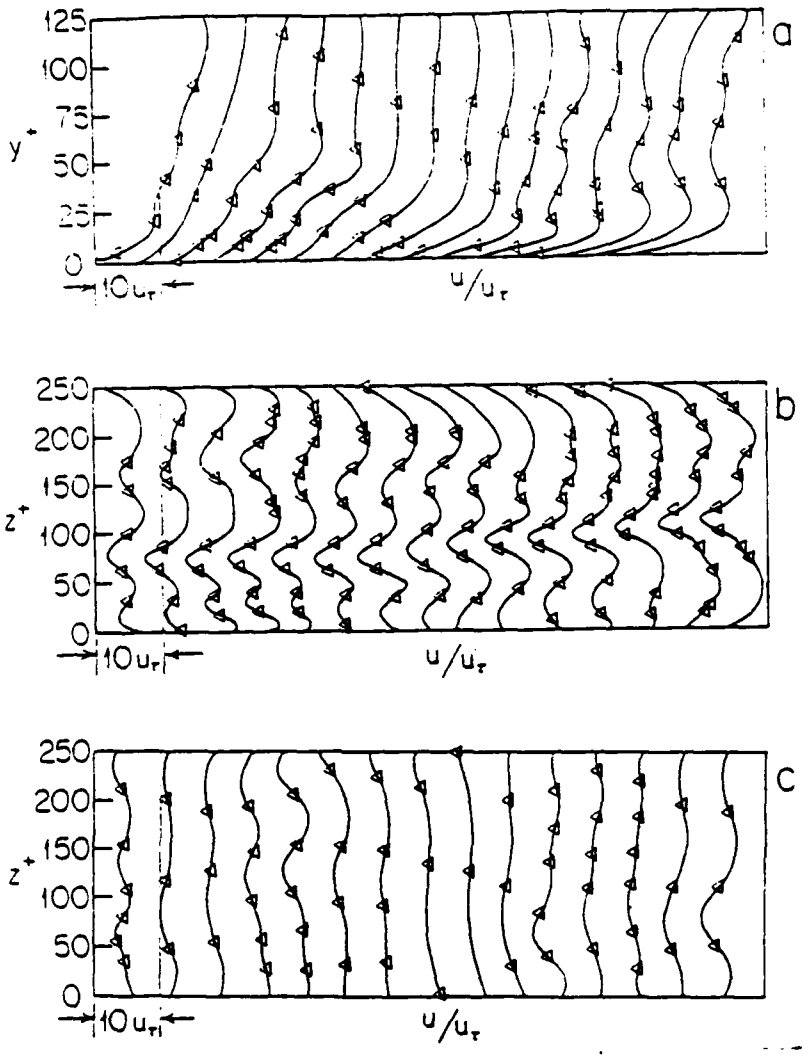

Fig. 11. **Instantaneous velocity profiles in the wall region from the direct numerical simulation of a turbulent channel flow in (a) the normal direction, (b) in the spanwise direction at $y^+ = 15$, and (c) in the spanwise direction at $y^+ = 66$. The inflection points are denoted by ◁ .**

state exists for the inflectional instability. Secondly the site of the instability should be far removed from a solid boundary to insure its inviscid character. Huerre (1983) has shown that the characteristics of the instability are hardly altered by the presence of a wall as long as the inflectional region is removed at least 1.2Δ from the wall. Since the length scale of the inflection is $5\text{-}10\nu/u_\tau^2$. Huerre's criteria appears to be satisfied for the inflections above $y^+ \cong 10$. The third condition necessary to apply the stability criteria is that of two-dimensionality. No theory is presently available to explain how this will effect the instability, but Nishioka et al's (1980) results discussed earlier suggest that the two-dimensional theory is valid in highly three-dimensional fields.

To determine the growth rates of the incipient instability, the data were explored further to obtain the strength of the shear layers associated with the inflectional profile. This was accomplished by first locating the position of the inflection points

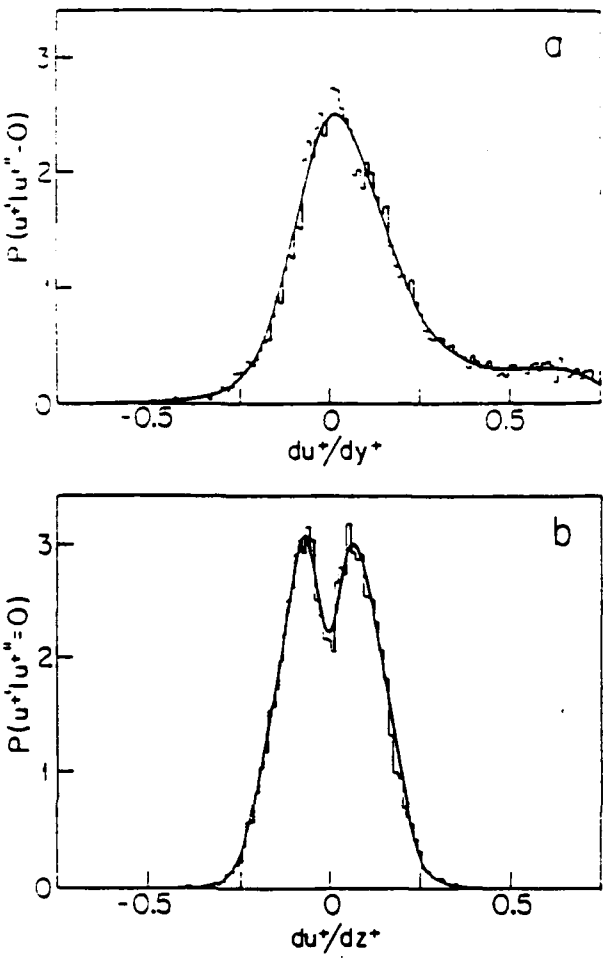

Fig. 12. **Conditional probability distribution of the velocity shear at the inflection points from experimental data with Re_θ = 2500. a) velocity shear perpendicular to the wall at $10 < y^+ < 20$. b) Velocity shear parallel to the wall at $y^+ = 15$.**

within a given spatial domain. All of the inflection points were included in the averaging process, although some could have been excluded using Fjørtoft's theorem. The value of the shear rate was then measured at each of these points. Thus the conditional probability of the shear rate could be obtained by sampling the shear at the points of inflection. The results are shown in figures 12 and 13 where the shear rates are normalized by the mean wall values. The first of these figures is obtained from the experimental hot-wire data base used in figure 10. The normal shear distribution in figure 12a is asymmetrical because of the mean shear in that direction. The most probable value of the shear is approximately zero and its mean value equals $\partial U/\partial y$ at that location. It is also interesting to note that the negative gradients are often observed as reported earlier by Willmarth and Sharma (1984). They also observed $\partial U/\partial y$ gradients which exceeded the mean shear at the wall. The corresponding spanwise shear in figure 12b is symmetrical as required and has dual peaks at a nondimensional shear of approximately ±0.1.

Numerical data obtained from Spalart (1987) were also analysed to compare with the experimental results. The same processing was used to obtain figure 13. The Reynolds number of this data is Re_θ = 670. The results are very similar to that in figure 12; the main difference being that the magnitudes of the probabilities are slightly lower and the distribution is slightly wider than in the experimental case. This difference may be due to the spatial averaging imposed by the hot-wires and the coarser grid spacing in the experimental case.

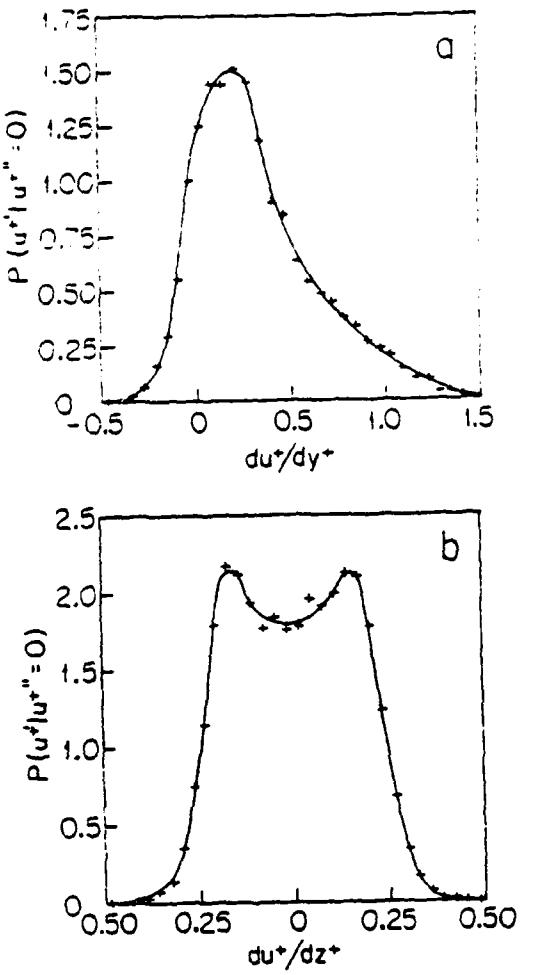

Fig. 13. **Similar results as in Figure 12 but for the direct numerical simulation of a turbulent boundary layer at $Re_\theta = 670$.**

If the inflectional profiles are indeed unstable, then one should be able to predict the wavelength of the amplified oscillation. Michalke's results suggest that the wavelength will be 15.7Δ. Close examination of figures 10 and 11 and other similar data indicate that Δ is roughly $10 \pm 5\nu/u_\tau$. Thus the inflectional profiles should produce disturbances with wavelengths between 75 and 225 ν/u_τ. Some distinct data exist in the literature which support this prediction. Dinkelacher et al. (1977) measured the pressure fluctuations on the wall and found wavelike patterns propogating downstream with wavelengths of $200\nu/u_\tau$ travelling at typically $12 - 15u_\tau$. Kline et al. (1967) also reported observations of wavelengths of $240\nu/u_\tau$. One reason there are few data of this type reported in the literature is that the oscillations are occurring within a random background and thus they are difficult to distinguish from the uncorrelated fluctuations. In addition, since the background provides the initial disturbance for the instability and the energy of the disturbance can grow by a factor of 1000 while travelling one wavelength downstream, an identifiable perturbation can probably only be observed for one or at most two wavelengths before it is distorted beyond the point of recognition.

DISCUSSION AND CONCLUSIONS

The primary result of this research is that inflectional velocity profiles are a prevalent and ubiquitous feature of the wall region of turbulent flow fields. The presence of low speed streaks in this region has been reported by numerous authors and is recognized as one of the clearest indications of the existence of wall layer eddy structures. The mere presence of low speed streaks is sufficient to guarantee that there will be inflectional velocity profiles in the spanwise direction because U(z) must vary from high to low values about a zero mean as seen in figures 9 through 11.

The instantaneous data also shows that there are numerous inflection points in the direction normal to the wall as well. This is somewhat surprising because of the restraining influence of the wall, but has been verified by different authors in several flows. The density of the $\partial^2U/\partial y^2 = 0$ points is comparable to the $\partial^2U/\partial z^2 = 0$ points in the region $10 < y^+ < 20$.

It is interesting to note that an "inflection point" is actually an intersection of a locus of such points. In the simplified two-dimensional tanh(y/Δ) profile, the locus of the inflection points is a plane at y = 0; i.e. an inflectional plane. The resulting instability waves have crests parallel to the inflectional plane with their crests aligned along the third axis, i.e. perpendicular to both the mean flow and to the direction of the gradient.. These waves are convected along the x axis. For the spatial growth case, the wave amplitude increases in x at each point in time.

In the three-dimensional cases considered here, the locus of inflection points will be a non-planar surface. For example, a wake has a locus of inflection points which forms a cylindrical surface aligned in the mean flow direction with equal amplitude of the shear, $\partial U/\partial \xi$, at every streamwise position. In fully developed turbulent flow, the inflectional surface is much more convoluted. For example, the side of a low speed streak will always be such a surface because $\partial^2U/\partial z^2 = 0$ there. If the streak has an inflectional U(y) profile, the inflectional surface may extend from one side of the low speed streak over its top to the other side engulfing the entire low speed region. If the strength of the shear $\partial U/\partial \xi$, is constant over the entire inflectional sheet, each instability wave will have a similar growth rate. The waves would be locally parallel to the inflectional sheet and hence would have the shape of a horseshoe. The vortices generated by Acarlar and Smith (1987ab) clearly illustrate this phenomenon in a well controlled laminar flow. Similar vortices were often observed in the transitional flow of Swearingen and Blackwelder (1987).

The inflectional surface is not necessarily of infinite extent. For example, a momentary disturbance at a point in a laminar boundary layer must have an inflectional surface of finite extent because the flow at large distances from the disturbance may be devoid of inflection points. In tracing out the inflectional surfaces in data such as in figures 10 and 11, one often sees that the surface ends abruptly at some point in the flow field although it may continue in the third dimension. In the turbulent case, the inflectional surfaces are random in space and time as well.

The locii of inflection points are important because they present a mechanism by which turbulence is produced. Namely the shear associated with the inflections is generally quite strong which suggests that an inviscid instability dominates the flow field. Through this mechanism, the unstable inflectional profiles can extract energy from the instantaneous base flow and produce a rapidly growing oscillation. The wavelength of the oscillation scales with the width of the inflectional instability. Since the scale of the inflections is random, so is the scale of the growing disturbance; however, the scale of all of the observed oscillations was well within the spectral domain of the turbulence. The instability grows extremely rapidly; i.e. the two-dimensional theory implies that the oscillations increase their amplitude by a factor of 30 (and its energy by 100) as it travels one wavelength downstream. The actual growth is probably tempered by energy spreading in the third dimension as well.

A model flow field emulating the turbulent wall region was studied which consisted of Görtler streamwise vortices in a laminar boundary. This flow had the advantage that it was steady and thus provided a better test bed for studying the velocity profiles and oscillations. Similar low speed streaks and inflectional profiles were observed in the model flow. Inflectional profiles in the normal and spanwise directions yielded regular and repeatable oscillations with wavelengths consistent with the predictions of Michalke (1965). The oscillations grew rapidly in the streamwise direction and broke down into turbulence after two to four wavelengths. In this flow field, it was clear that virtually all of the turbulence was produced by the inviscid instability. Not only were the dynamics similar between the model and turbulent flows but the length and velocity scales were also comparable when normalized with the friction velocity and the kinematic viscosity, as noted by Blackwelder(1983). This scaling is common in analyzing turbulent wall flows but has not been used frequently in transitional flows. The present results suggest that this scaling provides a means of comparing these two flow regimes in more detail than heretofore and indicates that their dynamics are indeed similar.

Finally, the evidence suggests that the instability may be more successful in producing u and w fluctuations than in producing u and v oscillations. Note that the instability will always produce an oscillation in the direction of the base flow, u. In a two-dimensional case, the second velocity component produced by the instability is the component parallel to the direction of the gradient. Since an inflection point is always present on the sides of the low speed streaks, one expects these to produce oscillations of u and w. Oscillations involving v may be less prevalent because inflections do not always occur above the low speed streak. However, it appears that by the time that large growth is observed, the locus of inflection points extends upward from the sides and over the low speed streak. In this case the observed oscillations will depend upon the integrated growth rates that the disturbances have experienced which may favor the spanwise oscillation since they have existed over a longer time period. In addition, the growth of the v oscillation will be hindered at some point by the presence of the wall, thus suggesting that the spanwise oscillations will dominate and produce a larger oscillation amplitude. This is of course consistent with the observations that $w' > v'$ in the wall region of turbulent shear flows.

All of the above are devoid of Reynolds averaging and its implications. In particular, these arguments view turbulent production as an instantaneous event related to a particular mechanism, e.g. the unstable inflectional velocity profile. The reported observations show that the growing oscillations are three dimensional and produce u, v, and w fluctuations in a random manner depending upon the orientation of the inflectional profile. This observation is not inconsistent with Reynolds averaging but does provide a different description of the production process. For example in the above formulation, the turbulent energy is fed directly into the u, v, and w fluctuations. The Reynolds averaged equations show that the average turbulent energy is only fed into the u fluctuations and then is redistributed by the pressure into the other components. The difference is that the averaged equations do not allow for instantaneous variations in the base flow, i.e. the mean averaged flow, whereas the instantaneous descriptions does.

ACKNOWLEDGEMENTS

The authors wish to thank Philippe Spalart for the use of his numerical boundary layer data and the Stanford-NASA/Ames Center for Turbulence Research for the opportunity to utilize the numerical data. The turbulent channel flow data base was provided by Richard Leighton and Robert Handler of the Naval Research Laboratory.

This research was supported by the Office of Naval Research under contract number N00014-82-K-0084 and the Air Force Office of Scientific Research through contract number F49620-85-C-0080. JDS thanks the National Research Council for their support through an NRC-NRL Research Associateship.

REFERENCES

Acarlar, M. S. and Smith, C. R., 1987a, "Haripin Vortices Generated by a Hemisphere Protuberance," Journal of Fluid Mechanics, 175, 1.

Acarlar, M. S. and Smith, C. R., 1987b, "Haripin Vortices Generated by Fluid Injection," Journal of Fluid Mechanics, 175, 43.

Bippes, H., 1972, "Experimentelle Untersuchung des laminar-turbulenten Umschlags an einer parallel angeströmten konkaven Wand," Sitzungsberischte der Heidelberger Akademie der Wissenschaften Mathematisch-naturwissenshaftliche Klasse, Jahrgang 1972, 3, 103.

Blackwelder, Ron F., 1983, "Analogies between Transitional and Turbulent Boundary Layers," Phys. Fluids, 26, 2807.

Blackwelder, R. F. and Eckelmann, H., 1979, "Streamwise Vortices Associated with the Bursting Phenomenon," Journal of Fluid Mechanics, 94, 577.

Cantwell, Brian J., 1981, "Organized Motion on Turbulent Flow", Ann. Rev. Fluid Mech., 13, 457.

Diprima, R. C. and Stuart, J. T., 1972, "Non-local Effects in the Stability of Flow Between Eccentric Rotating Cylinders," Journal of Fluid Mechanics, 54, 393.

Dinkelacher, A., Hessel, M., Meier, G. E. A. and Schewe, G., 1977, "Investigation of Pressure Fluctuations beneath a Turbulent Boundary Layer by Means of an Optical Method," Phys. Fluids, 20, S216.

Floryan, J. M. and Saric, W. S., 1982, "Stability of Görtler Vortices in Boundary Layers," A.I.A.A. Journal, 20, 316.

Gaster, M., Kit, E. and Wygnanski, I., 1985, "Large Scale Structures in a Forced Turbulent Mixing Layer," Journal of Fluid Mechanics, 150, 23.

Görtler, H., 1940, " Über eine dreidimensionale Instabilität laminarer Grenschichten an Konkaven Wänden," Nachr, Wiss, Ges. Göttingen, Math-Phys Kl, Neue Folge I, 2, 1.

Greenspan, H. P. and Benney, D. J., 1963, "On Shear Layer Instability and Breakdown," Journal of Fluid Mechanics, 15, 133.

Guezennec, Y., Piomelli, U. and Kim, J., 1987, "Asymmetric Characterization of Conditionally Averaged Structures in Wall Bounded Flows" Bulletin of American Physics Society, 32, 2046.

Hall P. (1983), "The Linear Development of Görtler Vortices in growing Boundary Layers" Journal of Fluid Mechanics, 130, 41.

Hall, Philip, 1987, "The Nonlinear Development of Görtler Vortices on Growing Boundary Layers," a manuscript.

Huerre, P., 1983, "Finite Amplitude Evolution of Mixing Layers on the Presence of Solid Boundaries," J. de Mecanique Theorique et appliquee, Numero Special, p. 121.

Kim, John and Moin, Parviz, 1986, "The Structure of the Vorticity Field in Turbulent Channel Flow, Part 2," Journal of Fluid Mechanics, 162, 339.

Kim, John, 1983, "On the Stucture of Wall-bounded Vortical Flows," Phy. Fluids, 26, 2088.

Kline, S. J., Reynolds, W.C., Schraub, F. A. and Runstadler, P.W., 1967, "The Structure of Turublent Boundary Layers," Journal of Fluid Mechanics, 30, 741.

Liepmann, H. W., 1945, "Investigation of Boundary Layer Stability and Transition on Concave Walls," NACA Wartime Report W-87.

Lin C. C., 1955, "The Theory of Hydrodynamical Stability," Cambridge University Press

Michalke, A., 1965, "On Spatially Growing Disturbances in an Inviscid Shear Layer," Journal of Fluid Mechanics, 23, 521.

Nishioka, M., Asai, M. and Iida, S., 1980, "An Experimental Investigation of the Secondary Instability," Laminar-Turbulent Transition, Ed. R. Eppler and H. Fasel, Springer Verlag, Berlin, p. 37.

Rayleigh, Lord, 1880, "On the Stability or Instability of Certain Fluid Motions," Proc. London Math Soc., 11, 57-70.

Sabry, A. S. and Liu, J. T. C., 1988, "Nonlinear Development of Görtler vortices and the Generation of High Shear Layers in the Boundary Layer," Proc. of Symposium in Honor of C. C. Lin, World Scientific Pub. Co., Singapore.

Smith, C. R. and Metzler, S. P., 1983, "The Characteristics of Low Speed Streaks in the Near Wall Region of a Turbulent Boundary Layer," Journal of Fluid Mechanics, 129, 27.

Smith, A. M. O., 1955, "On the Growth of Taylor-Görtler Vortices Along Highly Concave Walls,: Quat. Appl. Math, 13, 233.

Smith, C. R. and Schwartz, S. P., 1983, "Observation of Streamwise Rotation in the Near Wall Region of a Turbulent Boundary Layer," Phy. Fluids, 26, 641.

Spalart, Philippe, 1987, data provided through the Summer Program of the Center for Turbulence Research, Stanford-NASA/Ames.

Swearingen, J. D. and Blackwelder, R. F., 1987, "The Growth and Breakdown of Streamwise Vortices in the Presence of a Wall," Journal of Fluid Mechanics, 182, 255.

Willmarth, W. W. 1975, "Structure of Turbulence on Boundary Layers," Adv. Appl Mech., 15, 159.

Willmarth, W. W. and Sharma, L. K., 1984, "Study of Turbulent Structure with Hot-wires Smaller than the Viscous Length," Journal of Fluid Mechanics, 142, 121.